



Expression Analysis of Barrett's Esophagus-Associated High-Grade Dysplasia in Laser Capture Microdissected Archival Tissue

Citation

Sabo, E., P. A. Meitner, R. Tavares, C. L. Corless, G. Y. Lauwers, S. F. Moss, and M. B. Resnick. 2008. Expression analysis of Barrett's esophagus-associated high-grade dysplasia in laser capture microdissected archival tissue. *Clinical Cancer Research* 14(20): 6440–6448. doi:10.1158/1078-0432.CCR-08-0302

Published Version

doi:10.1158/1078-0432.CCR-08-0302

Permanent link

<http://nrs.harvard.edu/urn-3:HUL.InstRepos:32540834>

Terms of Use

This article was downloaded from Harvard University's DASH repository, and is made available under the terms and conditions applicable to Other Posted Material, as set forth at <http://nrs.harvard.edu/urn-3:HUL.InstRepos:dash.current.terms-of-use#LAA>

Share Your Story

The Harvard community has made this article openly available.
Please share how this access benefits you. [Submit a story](#).

[Accessibility](#)

Published in final edited form as:

Clin Cancer Res. 2008 October 15; 14(20): 6440–6448. doi:10.1158/1078-0432.CCR-08-0302.

Expression Analysis of Barrett's Esophagus Associated High Grade Dysplasia in Laser Capture Microdissected Archival Tissue

Edmond Sabo¹, Patricia A Meitner¹, Rosemarie Tavares¹, Christopher L Corless², Gregory Y Lauwers³, Steven F Moss⁴, and Murray B Resnick¹

¹Department of Pathology, Rhode Island Hospital/Brown University, Providence, RI, USA.

²Department of Pathology, Oregon Health & Science University, Portland, OR, USA.

³Department of Pathology, Massachusetts General Hospital, Boston, MA, USA.

⁴Department of Medicine, Rhode Island Hospital/Brown University, Providence, RI, USA.

Abstract

Purpose—Identifying genes differentially expressed in non-dysplastic Barrett's esophagus (BE) from those expressed in high grade dysplasia (HGD) should be of value in improving our understanding of this transition and may yield new diagnostic and/or prognostic markers. The aim of this study was to determine the differential transcriptome of HGD compared with non-dysplastic BE through gene microarray analysis of epithelial cells microdissected from archival tissue specimens.

Experimental Design—Laser capture microdissection (LCM) was used to isolate epithelial cells from adjacent inflammatory and stromal cells. Epithelial mRNA was extracted from areas of non-dysplastic BE and HGD in matched biopsies from 11 patients. mRNA was reverse transcribed and applied on Affymetrix cDNA microarray chips customized for formalin-exposed tissue. For a subset of these genes, differential gene expression was confirmed by RT-PCR and immunohistochemistry.

Results—There were 131 genes over-expressed by at least 2.5-fold in HGD versus non-dysplastic BE and 16 genes that were under-expressed by at least 2.5-fold. Among the over-expressed genes are several previously demonstrated to be increased in the neoplastic progression of BE, as well as novel genes such as lipocalin-2, S100A9, matrix metalloproteinase 12, secernin 1 and topoisomerase II α . Genes decreased in dysplastic epithelium include MUC5AC, trefoil factor1 (TFF1), meprin A and CD13. RT-PCR validated the changes in expression in 24 of 28 selected genes.

Immunohistochemistry confirmed increased protein expression for topoisomerase II α , S100A9 and lipocalin-2 and decreased expression of TFF1 across the spectrum of BE associated dysplasia from non-dysplastic BE through adenocarcinoma.

Address for reprint requests: Murray B. Resnick, MD/PhD, Pathology Department, APC12, Rhode Island Hospital, 593 Eddy St, Providence, RI 02903. Email: E-mail: mresnick@lifespan.org.

Statement of Clinical Relevance. Identification of biomarkers capable of distinguishing the grade of Barrett's esophagus-associated dysplasia, as well as identifying patients who are most likely to progress to adenocarcinoma would provide extremely valuable tools for both surgical pathologists and gastroenterologists. In this study we have identified a number of potential biomarkers using laser capture microdissection followed by gene expression profiling on archival clinical samples. As pathologists our primary goal was to identify candidates for the generation of immunohistochemical reagents as this technique is readily available in all pathology departments. A pilot study to determine the utility of using four of these as immunohistochemical markers showed that lipocalin-2, S100A9, TFF1 and especially topoisomerase II α all possess promising potential as indicators of BE-associated dysplasia. These proteins will need to be validated in a larger series of cases. We also identified a number of other potential candidates, many of which as yet do not have commercially available antibodies suitable for immunohistochemistry.

Conclusions—This is the first study to identify epithelial genes differentially expressed in HGD versus non-dysplastic BE in matched patient samples. The genes identified include several previously implicated in the pathogenesis of Barrett's-associated dysplasia and new candidates for further investigation.

Keywords

Barrett's esophagus; dysplasia; gene expression; laser capture microdissection (LCM); microarray

Introduction

Barrett's esophagus (BE) is a premalignant condition in which the normal squamous epithelium of the distal esophagus undergoes metaplasia to a specialized intestinal epithelium. The presence of BE increases the risk of developing esophageal adenocarcinoma (EAC); approximately 1% of patients diagnosed with BE will progress from metaplasia to dysplasia and finally to Barrett's related EAC (1,2). EAC are thought to develop from BE by way of a stepwise transition through low to high grade dysplasia (HGD). Approximately half of all patients with HGD will progress to EAC (3). Several genetic abnormalities have been implicated in the transition from BE through HGD to EAC including microsatellite instability (4), promoter hypermethylation (5-8) and altered expression of a large set of genes (reviewed by Fitzgerald) (9). The identification of HGD by light microscopy is still considered the gold standard by which patient follow-up and treatment is coordinated. However, the morphological distinction between LGD and HGD can be challenging (10,11). It would be beneficial to identify novel markers that would objectively differentiate the grade of dysplasia as well as identify patients irrespective of the degree of dysplasia who are more likely to progress to EAC. To date many molecular, immunohistochemical and other markers have been evaluated, however, none reliably distinguish between LGD and HGD or serve to predict progression of dysplasia to EAC (11).

Expressional profiling, which allows for the simultaneous examination of a large panel of genes is one method currently employed to search for novel biomarkers. DNA microarrays have been used to compare EAC, esophageal squamous cell carcinoma and BE and have identified unique gene expression profiles capable of discriminating between these entities (12-22). However, only one report has attempted to discriminate the transcriptome of BE associated dysplasia compared with non-dysplastic BE (22). Our study takes advantage of two technologies to allow for a more definitive comparison of the BE and HGD transcriptomes. One is laser capture microdissection (LCM) of HGD and BE to obtain purified populations of epithelial cells with minimal contaminating inflammatory and stromal cells. The second is the use of microarrays specifically designed for analyzing material from formalin-fixed paraffin embedded (FFPE) archival tissue specimens. Together, these technologies have allowed us to examine epithelium-specific changes that are related to the development of dysplastic BE.

Methods

Patients and Biopsies

Archival FFPE endoscopic esophageal biopsies that had been collected for clinical purposes were obtained from the Pathology Departments of the Rhode Island and Miriam Hospitals (Providence, RI), the Oregon Health and Science University Hospital (Portland, OR) and the Massachusetts General Hospital (Boston, MA) in accordance with Institutional Review Board approvals from all hospitals. Four micron sections were cut from each paraffin block and stained by hematoxylin and eosin. The slides were reviewed by experienced gastrointestinal pathologists (MR and either CC or GL) to confirm the presence of HGD and non-dysplastic BE. For gene array analysis, suitable cases had areas of both non-dysplastic BE as well as HGD

available for LCM and extraction of RNA. mRNA from a total of eleven paired biopsies was extracted for analysis on 22 microarray chips. For confirmation of representative genes of interest from the array results, additional biopsy samples from additional patients were laser captured for real time PCR and sectioned for immunohistochemistry.

Quality of RNA

Because of the potential for RNA degradation in the routinely collected and processed FFPE tissues it was important to check that the blocks contained RNA of suitable quality. Several 10 μ sections were cut from each paraffin block and total RNA was extracted and purified using a Paradise Quality Assessment Kit (KIT0313, Molecular Devices, Sunnyvale, CA). Genomic DNA was removed with RNase-Free DNase from the same kit. RNA was evaluated by an Agilent 2100 Bioanalyser using an RNA 6000 Nano LabChip kit (Agilent Technologies, Wilmington, DE) as described previously (23).

Laser Capture Microdissection and RNA Extraction

A Paradise FFPE Reagent System kit (KIT 0311, Molecular Devices) was used to extract and amplify RNA from laser-captured cells. In brief, 7 μ sections were air-dried, stained, dehydrated through graded alcohols and subjected to LCM within 2 h of deparaffinization. About 5000 surface epithelial cells each from areas of HGD and non-dysplastic BE were microdissected from the tissue sections and captured on LCM Macro Capsure caps (Molecular Devices) using an Autopix Automated LCM instrument (Molecular Devices). From the microdissected cells total RNA was extracted, purified and amplified through 1.5 rounds of linear amplification using T7 bacteriophage RNA polymerase-driven in vitro transcription. After first strand cDNA synthesis, quality of RNA was evaluated by real-time PCR, using primers for the 3' and 5' ends of β -actin. RNA was considered acceptable for analysis if the quantity of RNA was >15 ng and the 3':5' ratio for β -actin was < 10. The final amplification and labeling of the dsDNA product was done using an Enzo BioArray HighYield RNA Transcript Labeling Kit (Enzo Life Sciences, Farmingdale, NY).

Microarray Hybridization

Labeled cRNA was fragmented and then hybridized onto cDNA microarray chips customized for RNA extracted from FFPE tissues (human U133-X3P expression arrays, Affymetrix, Santa Clara, CA) at the Affymetrix Gene Chip Resource at the WM Keck Foundation Biotechnology Resource Laboratory (Yale University, New Haven, CT). These procedures have been described previously (23)

Bioinformatics and Statistical Methods

The expression signals were normalized using the Standardization and Normalization of Microarray Data (SNOMAD) web-based software (24). Concordantly absent expression signals were removed from the analysis. Statistical comparison of the gene expression levels between the two groups (HGD versus ND) was done using the Wilcoxon Matched-Pairs Signed-Ranks test using the SPSS statistical package for Windows (version 16.0, SPSS Inc., Chicago). In order to correct for the multiple hypotheses testing effect, q values were also calculated using the R open source statistical program with the q-value package (Bioconductor Software Project, Cambridge, MA). Gene annotation for classification of the genes in functional categories was done using the GenMAPP 2.0 (Gene MicroArray Pathway Profiler, Gladstone Institutes, 2000-2004, CA) and the web-based Database for Annotation, Visualization and Integrated Discovery (DAVID)¹ (25). The overall correlation of the fold changes between the Affymetrix chip and the PCR results was tested using the Spearman's

¹available at <http://david.abcc.ncifcrf.gov/>

coefficient of correlation. Two-tailed p values of 0.05 or less were considered to be statistically significant.

Confirmation of Microarray Results by Real-time PCR

Several genes of interest expressed at a >2.5-fold difference between non-dysplastic BE epithelium and HGD epithelium were selected for confirmation. CDNAs retained for gene of interest confirmation purposes were analyzed by real-time (RT)-PCR to verify the result from gene chip analysis. RT-PCR was performed on the 11 different paired samples per gene. Results were further confirmed by analysis of 17 new cases, eight of non-dysplastic BE and nine HGD. Whenever possible, gene-specific primers for RT-PCR were designed to span an intron (to rule out artefacts from genomic DNA contamination) and to amplify about 100 bp from within 400 bases of the 3' end of the gene because the Paradise kit employs oligo dT priming for first strand synthesis and formalin-fixed RNA is often fragmented to < 400 bases. Primers were designed using Primer3 shareware (26) and synthesized by Operon Technologies (Huntsville, AL). RT-PCR was accomplished on an MX4000 real-time instrument (Stratagene, Cedar Creek, TX) using Brilliant SYBR Green Master Mix reagents (Stratagene) according to the manufacturer's instructions. In parallel to measuring expression of genes of interest, reactions were performed using primers for the 3' end of the human β -actin gene, to which all data was then normalized. Amplification conditions yielded efficiencies greater than 90% and linear regression coefficients >0.990. β -actin was amplified from serial 10x dilutions of cDNA reverse transcribed from Stratagene Reference RNA and values were used to construct a calibration curve for each PCR run to relate the threshold cycle to the log input amount of template used and to determine relative amounts of gene transcripts. The sequence of each primer pair and the amplicon size are listed in Table 1. Thermocycling was carried out for 45 cycles, with denaturation at 95°C for 30 seconds, annealing for 1 min at 57°C, and extension at 72°C for 30 sec. All samples were run in duplicate. A dissociation temperature gradient was included at the end of each run to confirm absence of high molecular weight DNA and primer dimers.

Immunohistochemistry

Immunohistochemical analysis was performed on 12 additional biopsy samples from different patients with either non-dysplastic BE, HGD or adenocarcinoma and 11 samples of biopsies with low grade dysplasia (LGD). Topoisomerase II α staining was performed using a mAb (NeoMarkers, Fremont, CA) and lipocalin-2 a rat polyclonal Ab (R&D Systems, Minneapolis, MN). Antigen retrieval was performed by microwaving in citrate buffer pH6.0 for 10 minutes. Slides were blocked using Peroxidase-Blocking Reagent (Dako Corp., Carpinteria, CA). Primary antibody was diluted at 1:50 and incubated overnight at 4°C for topoisomerase II α and diluted at 1:1000 and incubated overnight at 4°C for lipocalin-2. For topoisomerase II α the Ab was detected using the Dako EnVision + Dual Link System Peroxidase (Dako) and the chromogen was developed using Dako Liquid DAB+ Substrate System. For lipocalin-2 the secondary Ab biotinylated anti-rat by Vector (Vector, Burlingame, CA) was incubated for 30 minutes. The Ab was detected using the VECTASTAIN ABC kit and the chromogen was developed using Dako Liquid DAB+ Substrate System. Immunohistochemistry for the pS2 mAb which recognizes TFF-1 (Zymed, Carlsbad, CA) and the S100A9 mAb (Novus Biologicals, Littleton, CO), was performed on the Ventana Discovery System (Ventana, Tucson AZ) using CC1 antigen retrieval. Ab dilutions were 1:25 and 1:100 respectively. The antibodies were developed using the DAB MAP kit (Ventana). The slides were counterstained using hematoxylin, dehydrated and coverslipped.

Positive controls included normal squamous mucosa which stains strongly for both lipocalin-2 and S100A9, normal gastric cardia which stains strongly for TFF-1, and basal cells of squamous mucosa and glandular crypt cells which stain for topoisomerase II α . We used the following

scoring system based on the extent of staining of the superficial aspects of the non-dysplastic and dysplastic BE mucosa and adenocarcinoma. Negative to weak staining; 0-10% staining = 1, moderate; 10-50% = 2, and strong; 50-100% = 3. The association between the diagnostic categories (NDBE, LGD, HGD, ADCA) and the immunohistochemical staining binarized scores (negative to low versus moderate to high), were tested using the Chi square test. Two-tailed p values of 0.05 or less were considered to be statistically significant.

Results

Expression Array Analysis of Dysregulated Epithelial Genes in Barrett's Esophagus High Grade Dysplasia

After removing the concordantly absent microarray signals, 7990 transcripts decreased and 14,562 increased in the HGD group as compared to the non-dysplastic BE group. Applying a statistical threshold of $p < 0.05$ and $q < 1$ led to a final list of 147 genes of interest. Multiple gene function categories were represented in this list of differentially expressed genes including genes involved in calcium binding and ion channels, cell adhesion, motility and membrane proteins, cell proliferation and cell death, extracellular matrix and protease, metabolism and mitochondria and others (Figure 1). A list of the 147 genes divided into these categories as well as a full list of all differentially expressed genes and their expressed signals are available as supplementary data (see addendum Tables A and B respectively).

Confirmation of Selected Genes by RT-PCR

Real-time quantitative PCR was used to verify changes in those genes whose expression according to the microarray analysis showed the greatest differential expression between non-dysplastic BE and HGD (16 upregulated and 11 downregulated), (Table 2). One other gene (S100A9) of potential interest as an immunohistochemical marker of BE associated dysplasia was also evaluated. For this study, certain genes were excluded if they were from uncharacterized or partially characterized proteins or if they were not previously shown to be expressed by epithelial cells based on our search of the current literature in the National Library of Medicine PubMed database². In the vast majority of genes tested (24 of 28) there was agreement in terms of increase or decrease between microarray data and the RT-PCR data (Figure 2). In the case of testisin, osteoglycin, sucrase-isomaltase and the t(12;16) fusion gene *FUS..CHOP*, the amplification signal was very low (either not detected at all or only detected in some of the tissue samples).

Confirmation of Selected Genes by Immunohistochemistry

Immunohistochemical analysis was performed on three proteins, topoisomerase II α , S100A9, and lipocalin-2 whose expression was shown to be greatly increased by microarray analysis in HGD epithelium and one protein, trefoil factor 1 (TFF-1), whose expression was decreased in areas of HGD. Staining was performed on 12 sections of non-dysplastic BE, HGD and adenocarcinoma and 11 sections of LGD, all from additional patient samples not used for the microchip analysis. Topoisomerase II α strongly stained the nuclei of the luminal surface epithelial cells from areas of HGD (Figure 3A). Five HGD cases exhibited a strong staining pattern (over 50% of nuclei stained) and seven a moderate (10-50%) staining pattern (Figure 4). In the biopsies of non-dysplastic BE occasional nuclear staining was evident in the proliferative crypt region varying in numbers from 10-40% of the crypt nuclei, however, only rare (<1%) surface epithelial staining was identified (Figure 3B). The extent of staining of the low grade cases was intermediate as compared to the control cases whereas there was no

²<http://www.ncbi.nlm.nih.gov/>

significant difference between staining of the HGD cases and the adenocarcinoma cases (Figure 4).

The pattern of S100A9 staining was both nuclear and cytoplasmic. Of the 12 cases of HGD examined, moderate staining was seen in five cases, however, the extent of staining was patchy involving between 10-50% of the dysplastic epithelium. (Figure 3C, Figure 4). Seven other cases of HGD exhibited negative to focal weak staining pattern. S100A9 staining was also seen in lamina propria inflammatory cells (Figure 3C). None of the non-dysplastic BE epithelium exhibited staining for S100A9 (Figure 3D). The extent of staining of the LGD was no different than the HGD cases, however, significantly more staining was seen in adenocarcinomas than the HGD (Figure 4).

Similar to the S100A9 staining pattern, staining of the dysplastic epithelium with lipocalin-2 was variable. Moderate to strong cytoplasmic staining was seen in seven of twelve cases examined (Figure 3E, Figure 4), however, the staining was negative to focal in the five remaining cases. Eleven of the twelve non-dysplastic BE were negative for lipocalin-2 (Figure 3F, Figure 4). There were no significant differences between the extent of staining of the HGD and the LGD or adenocarcinoma cases. Eleven of the twelve HGD biopsies were negative for TFF-1 (Figure 3G, Figure 4), whereas one case exhibited strong diffuse cytoplasmic staining pattern. All of the non-dysplastic BE epithelium tested demonstrated strong diffuse cytoplasmic staining for TFF-1 (Figure 3H, Figure 4). The extent of staining of the HGD cases was significantly different than the LGD but not different than the adenocarcinomas (Figure 4).

Discussion

Identifying genes differentially expressed in BE without dysplasia from those expressed in BE with HGD should be of value in improving our understanding of this transition, and genes might also prove to be of diagnostic and of prognostic utility. Screening for biomarkers using cDNA microarray expression technologies is a powerful means to obtain a genome wide assessment of differential gene expression. Although a number of cDNA microarray studies have been conducted comparing the differential gene expression of esophageal adenocarcinomas to normal esophageal mucosa or to non-dysplastic BE (12-22) only one other microarray study specifically compared gene expression of BE with HGD to non-dysplastic BE mucosa (22). The study by Bax et al examined the expression profile of paired whole biopsy (as opposed to LCM epithelium) samples of HGD and non-dysplastic BE from only one patient although the expression of upregulated genes was confirmed in additional patient samples. Other than being the second study to specifically compare the transcriptome of HGD to non-dysplastic BE, our study is the first to utilize LCM in order to concentrate on genes expressed only by the neoplastic epithelium and the only study to utilize FFPE tissues for this purpose.

Using a 2.5 fold threshold we identified a total of 131 upregulated and 16 downregulated genes in HGD epithelium and verified a number of these dysregulated genes by RT-PCR on the original biopsy material and additional tissue samples. The correlation between the chip and RT-PCR was excellent confirming that this technology is a viable application for future biomarker discovery. Since T7 bacteriophage RNA polymerase-driven linear amplification of RNA was used for the chip analysis, it is not surprising that the absolute fold values did not agree completely between the gene microarray data and the follow-up RT-PCR studies. Just four dysregulated genes could not be confirmed, probably because they were expressed at levels below detection in some of our FFPE tissues.

Our study identified a number of genes previously described as being modified in the progression of BE through EAC as well as several novel genes. Bax et al also reported that

expression of the calcium binding protein S100A9 (calgranulin B) was consistently upregulated in HGD (22). S100A9 is expressed by neutrophils and monocytes and is thought to be involved in chemotaxis (27), however, it has also been shown to be expressed by certain epithelial cells where its function has been linked to cell proliferation (28). Four genes, two of which were upregulated — (ADAMTS12 and pleckstrin homology-like family domain A) and two downregulated — (sucrose isomaltase and fatty acid binding protein 1), were also identified by Helm et al as candidate gene predictors of progression to EAC in BE (19). Both collagenase (MMP1) and metalloelastase (MMP12) have been shown to be upregulated in the epithelium of BE associated adenocarcinoma, however, a component of this increased expression may be related to macrophages and other inflammatory cells (29). Several additional genes that we found to be downregulated in HGD — (TFF-1, MUC5AC, meprin A, CD13 and sucrose isomaltase) were also found by others to be decreased in BE associated neoplasia (22,30-33). MUC5AC is a gastric type mucin expressed by non-dysplastic BE epithelium (31) whose expression pattern has been shown to be altered during neoplastic progression (33). The trefoil protein TFF-1 which is thought to play a role as a tumor suppressor gene in gastric carcinoma has been shown by Fox et al to be lost late in the progression of BE to EAC (32) and was decreased in HGD in the study by Bax (22). Meprin A is a protease known to cleave extracellular matrix components in vitro, and thus may contribute to tumor progression by facilitating migration, intravasation, and metastasis of carcinoma cells (30). Interestingly in our study and in the study by Fox et al (32) meprin A was shown to be downregulated in EAC, suggesting this protease may be involved in processes other than extracellular matrix degradation in BE associated neoplastic progression. Finally, Fox et al also described decrease expression of the microsomal aminopeptidase CD13 and the enzyme sucrose isomaltase in EAC as compared to non-dysplastic BE (32).

One goal of our study was to identify potential immunohistochemical biomarkers for HGD which would be suitable for use on endoscopic FFPE biopsy material. Commercial antibodies developed for FFPE tissue were available for three proteins that we found to be highly upregulated in HGD and one downregulated protein. Topoisomerase II α is an enzyme required for DNA replication which has been previously shown to be increased in gastrointestinal cancers (stomach, colon and esophagus) (34-36) however, its expression has not been studied in BE or BE associated dysplasia. Here we show that topoisomerase II α mRNA expression was increased 12 fold in regions of HGD. By immunohistochemistry topoisomerase II α nuclear staining extended from the proliferative region up to the surface dysplastic epithelial cells in cases of both LGD and HGD in a pattern similar to that described for the proliferative marker Ki-67 (37,38). It remains to be seen whether topoisomerase staining will be superior to Ki-67 in differentiating LGD from HGD, or BE with reactive changes from dysplasia, as well as whether it predicts progression of dysplasia to adenocarcinoma. Lipocalin-2 is a cell survival factor (39) which has been shown to be upregulated in pancreatic, breast and ovarian cancer (40-42) and more recently in gastric cancer (43) and esophageal squamous carcinoma (44). It is expressed both by epithelial cells and inflammatory cells primarily neutrophils. The extent of immunohistochemical staining for both lipocalin-2 and S100-A9 in the HGD biopsies sampled was patchier than that observed for topoisomerase suggesting that these two proteins may be less useful as markers of HGD. Interestingly, the extent of staining of S100-A9 was greater in the adenocarcinomas than in the HGD cases suggesting that this protein may be used as a marker for progression. Loss of staining for TFF-1 was seen in the majority of HGD biopsy tested and albeit a negative marker suggests that TFF-1 may be useful in the diagnosis of HGD in challenging cases. Loss of TFF-1 was also seen in about half of the cases of LGD suggesting that this is an early event in neoplastic progression of BE to adenocarcinoma. Based on this limited study it appears that only topoisomerase II α may be useful in differentiating HGD from LGD, however, we are planning to extend this pilot study to include additional cases and also examine whether any of these markers are capable of predicting progression of BE with or without dysplasia to adenocarcinoma.

We identified a number of potential biomarkers for HGD for which antibodies suitable for FFPE tissues do not as yet exist. Secernin expression was highly increased in HGD has been recently shown to be upregulated in gastric cancer (45). Gastrointestinal glutathione peroxidase (GPx2) is highly expressed in the proliferative area of the intestinal crypt (46) and upregulated during the development of colon cancer (47) and has been recently been shown to be expressed by BE (48), however, nothing is known about its expression in BE associated dysplasia or adenocarcinoma. Glial cell line derived neurotrophic factor (GDNF) receptor is a ligand for a polypeptide which promotes neuronal survival has also been shown to be upregulated in bile duct and pancreatic carcinomas (49,50). Hydroxyprostaglandin dehydrogenase 15 (*HPGD*) which was downregulated in HGD as opposed to non-dysplastic BE mucosa is a putative tumor suppressor in lung carcinoma which may act by decreasing the levels of proliferative prostaglandin E2 (51).

In summary, we have shown that with careful selection of tissue blocks and attention to ensuring a high quality of extracted RNA it is possible to uncover the global gene expression profile of esophageal epithelial cells from FFPE archival tissue. Recent studies have shown that similar techniques have been successfully performed on breast, gastric, colonic, and prostatic epithelium suggesting that this methodology is a powerful means for screening of new biomarkers (23,52-54). As pathologists our primary goal was to identify candidates for the generation of immunohistochemical reagents as immunohistochemistry is available in all pathology departments and all pathologists are quite comfortable with the technique. Theoretically real-time PCR could be used as an adjunct technique on morphologically equivocal cases, however, this would probably require laser capture microdissection, a technique that is quite labor intensive and not universally available in most pathology departments.

Supplementary Material

Refer to Web version on PubMed Central for supplementary material.

Acknowledgements

We would like to thank Shrikant Mane and Sheila Westman at the Yale/Keck Foundation Affymetrix GeneChip Facility for helpful discussions and assistance with microarray hybridizations.

Financial Support: This project was supported by the Molecular Pathology Core of the COBRE Center for Cancer Research Development, NIH #P20 RR17695, awarded by the National Center for Research Resources, Institutional Development Award (IDeA) Program.

References

1. O'Connor JB, Falk GW, Richter JE. The incidence of adenocarcinoma and dysplasia in Barrett's esophagus: report on the Cleveland Clinic Barrett's Esophagus Registry. *Am J Gastroenterol* 1999;94:2037-42. [PubMed: 10445525]
2. Shaheen N, Ransohoff DF. Gastroesophageal reflux, Barrett esophagus and esophageal cancer. *JAMA* 2002;287:1972-81. [PubMed: 11960540]
3. Levine DS. Management of dysplasia in the columnar-lined esophagus. *Gastroenterol Clin North Am* 1997;26:613-34. [PubMed: 9309409]
4. Meltzer SJ, Yin J, Manin B, et al. Microsatellite instability occurs frequently and in both diploid and aneuploid cell populations of Barrett's-associated esophageal adenocarcinomas. *Cancer Res* 1994;54:3379-82. [PubMed: 8012954]
5. Klump B, Hsieh CJ, Holzmann K, Gregor M, Porschen R. Hypermethylation of the CDKN2/p16 promoter during neoplastic progression in Barrett's esophagus. *Gastroenterology* 1998;115:1381-6. [PubMed: 9834265]

6. Eads CA, Lord RV, Kurumboor SK, et al. Fields of aberrant CpG island hypermethylation in Barrett's esophagus and associated adenocarcinoma. *Cancer Res* 2000;60:5021–6. [PubMed: 11016622]
7. Lee OJ, Schneider-Stock R, McChesney PA, et al. Hypermethylation and loss of expression of glutathione peroxidase-3 in Barrett's tumorigenesis. *Neoplasia* 2005;7:854–61. [PubMed: 16229808]
8. Clement G, Braunschweig R, Pasquier N, Bosman FT, Benhattar J. Methylation of APC, TIMP3, and TERT: a new predictive marker to distinguish Barrett's oesophagus patients at risk for malignant transformation. *J Pathol* 2006;208:100–7. [PubMed: 16278815]
9. Fitzgerald RC. Molecular basis of Barrett's oesophagus and oesophageal adenocarcinoma. *Gut* 2006;55:1810–20. [PubMed: 17124160]
10. Montgomery E, Bronner MP, Goldblum JR, et al. Reproducibility of the diagnosis of dysplasia in Barrett esophagus: a reaffirmation. *Hum Pathol* 2001;32:368–78. [PubMed: 11331953]
11. Selaru FM, Zou T, Xu Y, et al. Global gene expression profiling in Barrett's esophagus and esophageal cancer: a comparative analysis using cDNA microarrays. *Oncogene* 2002;21:475–478. [PubMed: 11821959]
12. Odze RD. Diagnosis and grading of dysplasia in Barrett's oesophagus. *J Clin Pathol* 2006;59:1029–38. [PubMed: 17021130]
13. Xu Y, Selaru FM, Yin J, et al. Artificial neural networks and gene filtering distinguish between global gene expression profiles of Barrett's esophagus and esophageal cancer. *Cancer Res* 2002;62:3493–7. [PubMed: 12067993]
14. Barrett MT, Yeung KY, Ruzzo WL, et al. Transcriptional analyses of Barrett's metaplasia and normal upper GI mucosae. *Neoplasia* 2002;4:121–8. [PubMed: 11896567]
15. Dahlberg PS, Ferrin LF, Grindle SM, Nelson CM, Hoang CD, Jacobson B. Gene expression profiles in esophageal adenocarcinoma. *Ann Thorac Surg* 2004;77:1008–15. [PubMed: 14992916]
16. Hansel DE, Dhara S, Huang RC, et al. CDC2/CDK1 expression in esophageal adenocarcinoma and precursor lesions serves as a diagnostic and cancer progression marker and potential novel drug target. *Am J Surg Pathol* 2005;29:390–399. [PubMed: 15725809]
17. Gomes LI, Esteves GH, Carvalho AF, et al. Expression profile of malignant and non-malignant lesions of esophagus and stomach: differential activity of functional modules related to inflammation and lipid metabolism. *Cancer Res* 2005;65:7127–7136. [PubMed: 16103062]
18. Kimchi ET, Posner MC, Park JO, et al. Progression of Barrett's metaplasia to adenocarcinoma is associated with the Suppression of the transcriptional programs of epidermal differentiation. *Cancer Res* 2005;65:3146–54. [PubMed: 15833844]
19. Helm J, Enkemann SA, Coppola D, Barthel JS, Kelley ST, Yeatman TJ. Dedifferentiation precedes invasion in the progression from Barrett's metaplasia to esophageal adenocarcinoma. *Clin Cancer Res* 2005;11:2478–85. [PubMed: 15814623]
20. Hao Y, Triadafilopoulos G, Sahbaie P, Young HS, Omary MB, Lowne AW. Gene expression profiling reveals stromal genes expressed in common between Barrett's esophagus and adenocarcinoma. *Gastroenterology* 2006;131:925–933. [PubMed: 16952561]
21. Greenawalt DM, Duong C, Smyth GK, et al. Gene expression profiling of esophageal cancer: comparative analysis of Barrett's esophagus, adenocarcinoma, and squamous cell carcinoma. *Int J Cancer* 2007;120:1914–21. [PubMed: 17236199]
22. Bax DA, Siersema PD, Haringsma J, et al. High-grade dysplasia in Barrett's esophagus is associated with increased expression of calgranulin A and B. *Scand J Gastroenterol* 2007;42:902–10. [PubMed: 17613918]
23. Resnick MB, Sabo E, Meitner PA, et al. Global analysis of the human gastric epithelial transcriptome altered by *Helicobacter pylori* eradication in vivo. *Gut* 2006;55:1717–24. [PubMed: 16641130]
24. Colantuoni C, Henry G, Zeger S, Pevsner J. SNOMAD (Standardization and Normalization of MicroArray Data): web-accessible gene expression data analysis. *Bioinformatics* 2002;18:1540–1. [PubMed: 12424128]
25. Dennis G, Sherman BT, Hosack DA, et al. DAVID: Database for Annotation, Visualization, and Integrated Discovery, rev. 2007. *Genome Biol* 2003;4(9):R60.Epub 2003 August 14
26. Rozen, S.; Skaletsky, HJ. Primer3 on the WWW for general users and for biologist programmers. In: Krawetz, S.; Misener, S., editors. *Bioinformatics Methods and Protocols: Methods in Molecular Biology*. Humana Press; Totowa, NJ: 2000. p. 365–386.

27. Ryckman C, Vandal K, Rouleau P, Talbot M, Tessier PA. Proinflammatory activities of S100: proteins S100A8, S100A9 and S100A8A9 induce neutrophil chemotaxis and adhesion. *J Immunol* 2003;171:2602–09. [PubMed: 12928412]
28. Broome AM, Ryan D, Eckert RL. S100 protein subcellular localization during epidermal proliferation and psoriasis. *Histochem Cytochem* 2003;51:675–685.
29. Salmela MT, Karjalainen-Lindsberg ML, Puolakkainen P, Saarialho-Kere U. Upregulation and differential expression of matrilysin (MMP-7) and metalloelastase (MMP-12) and their inhibitors TIMP-1 and TIMP-3 in Barrett's oesophageal adenocarcinoma. *Br J Cancer* 2001;85:383–92. [PubMed: 11487270]
30. Lottaz D, Maurer CA, Hahn D, Büchler MW, Sterchi EE. Nonpolarized secretion of human meprin α in colorectal cancer generates an increased proteolytic potential in the stroma. *Cancer Res* 1999;59:1127–33. [PubMed: 10070973]
31. Warson C, Van Der Bovenkamp JH, Korteland-Van Male AM, et al. Barrett's esophagus is characterized by expression of gastric-type mucins (MUC5AC, MUC6) and TFF peptides (TFF1 and TFF2), but the risk of carcinoma development may be indicated by the intestinal-type mucin, MUC2. *Hum Pathol* 2002;33:660–8. [PubMed: 12152167]
32. Fox CA, Sapinoso LM, Zhang H, et al. Altered expression of TFF-1 and CES-2 in Barrett's esophagus and associated adenocarcinomas. *Neoplasia* 2005;7:407–416. [PubMed: 15967118]
33. Glickman JN, Blount PL, Sanchez CA, et al. Mucin core polypeptide expression in the progression of neoplasia in Barrett's esophagus. *Hum Pathol* 2006;37:1304–15. [PubMed: 16949933]
34. Kim R, Ohi Y, Toge T. Expression and relationship between topoisomerase I and II α genes in tumor and normal tissues in esophageal, gastric and colon cancers. *Anticancer Res* 1999;19:5393–8. [PubMed: 10697567]
35. Staley BE, Samowitz WS, Bronstein IB, Holden JA. Expression of DNA topoisomerase I and DNA topoisomerase II α in carcinoma of the colon. *Mod Pathol* 1999;12:356–61. [PubMed: 10229499]
36. Kanta SY, Yamane T, Dobashi Y, Mitsui F, Kono K, Ooi A. Topoisomerase II α gene amplification in gastric carcinomas: correlation with the HER2 gene. *Hum Pathol* 2006;37:1333–1343. [PubMed: 16949920]
37. Reid BJ, Sanchez CA, Blount PL, Levine DS. Barrett's esophagus: cell cycle abnormalities in advancing stages of neoplastic progression. *Gastroenterology* 1993;105:119–29. [PubMed: 8514029]
38. Hong MK, Laskin WB, Herman BE, Johnston MH, et al. Expansion of the Ki-67 proliferative compartment correlates with degree of dysplasia in Barrett's esophagus. *Cancer* 1995;75:423–9. [PubMed: 7812911]
39. Tong Z, Wu X, Ovcharenko D, Zhu J, Chen CS, Kehrner JP. Neutrophil gelatinase-associated lipocalin as a survival factor. *Biochem J* 2005;391:441–448. [PubMed: 16060857]
40. Argani P, Rosty C, Reiter RE, et al. Discovery of new markers of cancer through serial analysis of gene expression: prostate stem cell antigen is overexpressed in pancreatic adenocarcinomas. *Cancer Res* 2001;61:4320–4324. [PubMed: 11389052]
41. Santin AD, Zhan F, Bellone S, et al. Gene expression profiles in primary ovarian serous papillary tumors and normal ovarian epithelium: identification of candidate molecular markers for ovarian cancer diagnosis and therapy. *Int J Cancer* 2004;112:14–25. [PubMed: 15305371]
42. Fernandez CA, Yan L, Louis G, Yang J, Kutok JL, Moses MA. The matrix metalloproteinase-9/neutrophil gelatinase A associated lipocalin complex plays a role in breast tumor growth and is present in the urine of breast cancer patients. *Clin Cancer Res* 2005;11:5390–5395. [PubMed: 16061852]
43. Kubben FJ, Sier CF, Hawinkels LJ, et al. Clinical evidence for a protective role of lipocalin-2 against MMP-9 autodegradation and the impact for gastric cancer. *Eur J Cancer* 2007;43:1869–1876. [PubMed: 17604154]
44. Zhang H, Xu L, Xiao D, et al. Upregulation of neutrophil gelatinase-associated lipocalin in oesophageal squamous cell carcinoma: significant correlation with cell differentiation and tumour invasion. *J Clin Pathol* 2007;60:555–61. [PubMed: 17412867]
45. Suda T, Tsunoda T, Uchida N, et al. Identification of secernin 1 as a novel immunotherapy target for gastric cancer using the expression profiles of cDNA microarray. *Cancer Sci* 2006;97:411–19. [PubMed: 16630140]

46. Chu FF, Doroshow JH, Esworthy RS. Expression, characterization and tissue distribution of a new selenium dependent glutathione peroxidase GSHPx-GI. *J Biol Chem* 1993;8:2571–6. [PubMed: 8428933]
47. Al-Taie OH, Uceyler N, Eubner U, et al. Expression profiling and genetic alterations of the selenoproteins GI-GPx and SePP in colorectal carcinogenesis. *Nutr Cancer* 2004;48:6–14. [PubMed: 15203372]
48. Mork H, Scheurlen M, Al-Taie O, et al. Glutathione peroxidase isoforms as part of the local antioxidative defense system in normal and Barrett's esophagus. *Int J Cancer* 2003;105:300–304. [PubMed: 12704661]
49. Iwahashi N, Nagasaka T, Tezel G, et al. Expression of glial cell-line derived neurotrophic factor correlates with perineural invasion of bile duct carcinoma. *Cancer* 2002;94:167–174. [PubMed: 11815973]
50. Ito Y, Okada Y, Sato M, et al. Expression of glial cell-line derived neurotrophic factor family members and their receptors in pancreatic cancers. *Surgery* 2005;138:788–794. [PubMed: 16269310]
51. Ding Y, Tong M, Liu S, Moscow JA, Tai HH. NAD⁺ linked hydroxyprostaglandin dehydrogenase (15-PGDH) behaves as a tumor suppressor in lung cancer. *Carcinogenesis* 2005;26:65–72. [PubMed: 15358636]
52. Ma XJ, Wang Z, Ryan P, et al. A two-gene expression ratio predicts clinical outcome in breast cancer patients treated with tamoxifen. *Cancer Cell* 2004;5:607–616. [PubMed: 15193263]
53. Coudry RA, Meirless SI, Stoyanova R, et al. Successful application of microarray technology to microdissected formalin-fixed paraffin embedded tissues. *J Mol Diag* 2007;9:70–9.
54. Furusato B, Shaheduzzaman S, Petrovics G, et al. Transcriptome analyses of benign and malignant prostate epithelial cells in formalin-fixed paraffin embedded whole mounted radical prostatectomy specimens. *Prostate Cancer Prostatic Dis.* 2007(Epub ahead of print)

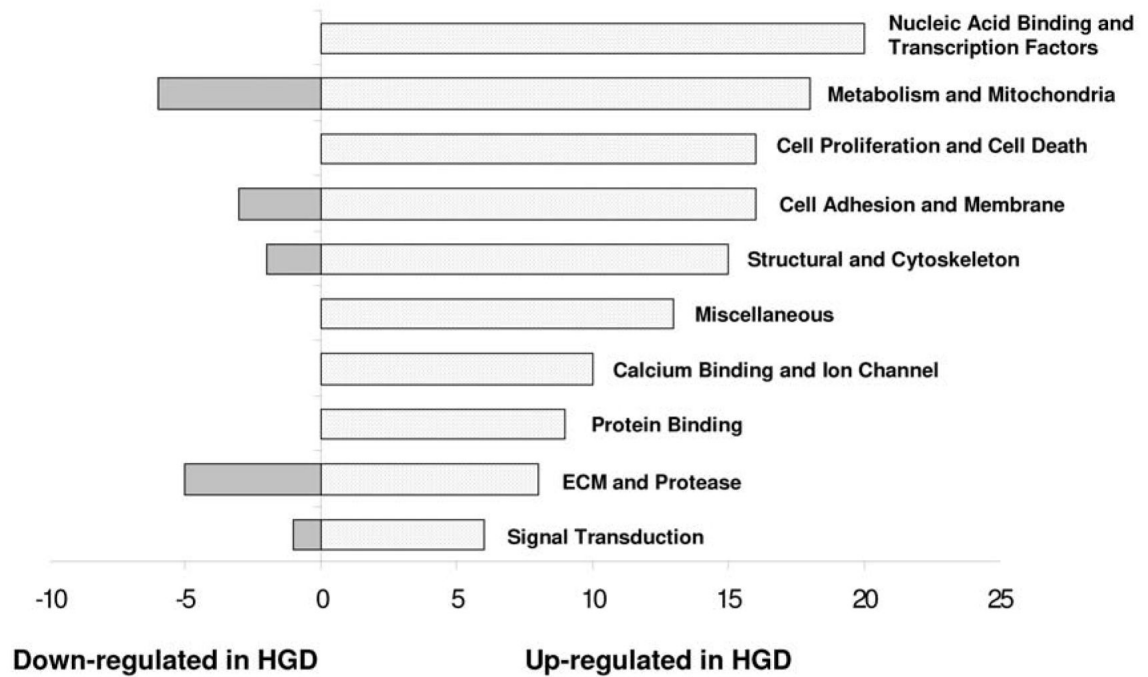


Figure 1.
Differentially expressed genes in high grade dysplasia (HGD) divided into functional categories.

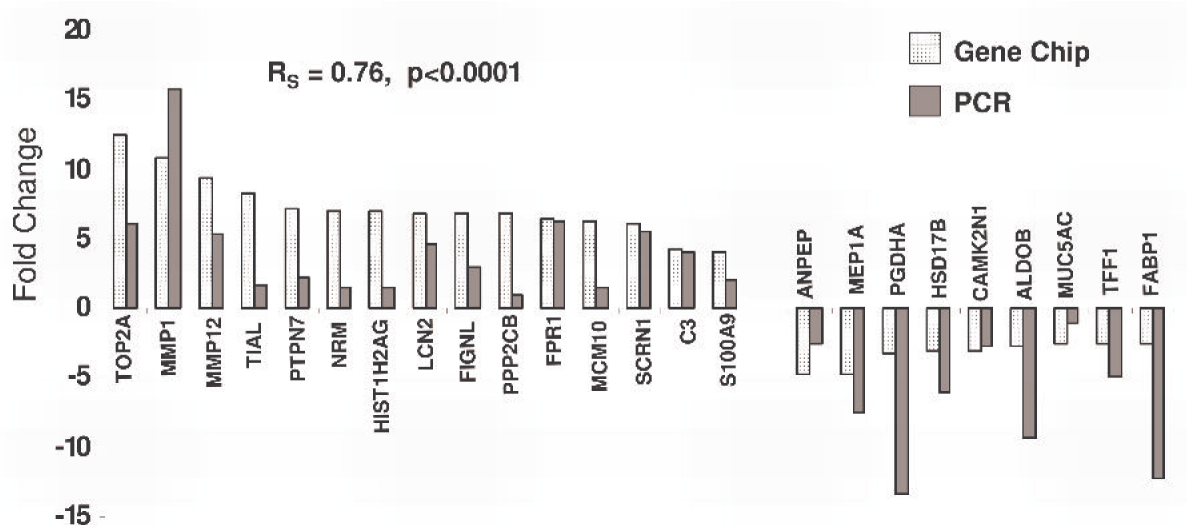


Figure 2.
Confirmation of the expression levels of selected dysregulated genes by RT-PCR and correlation with microarray data.

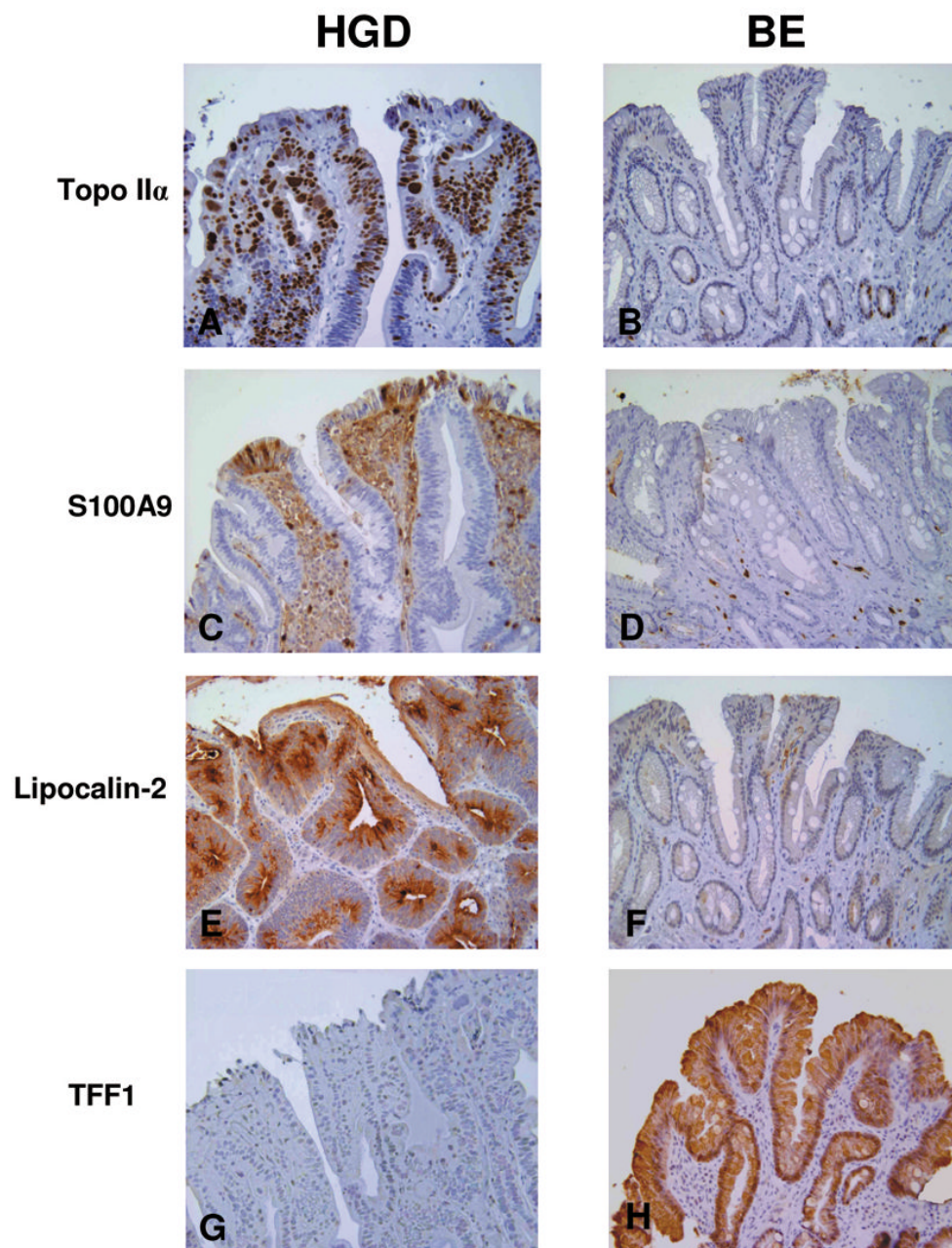
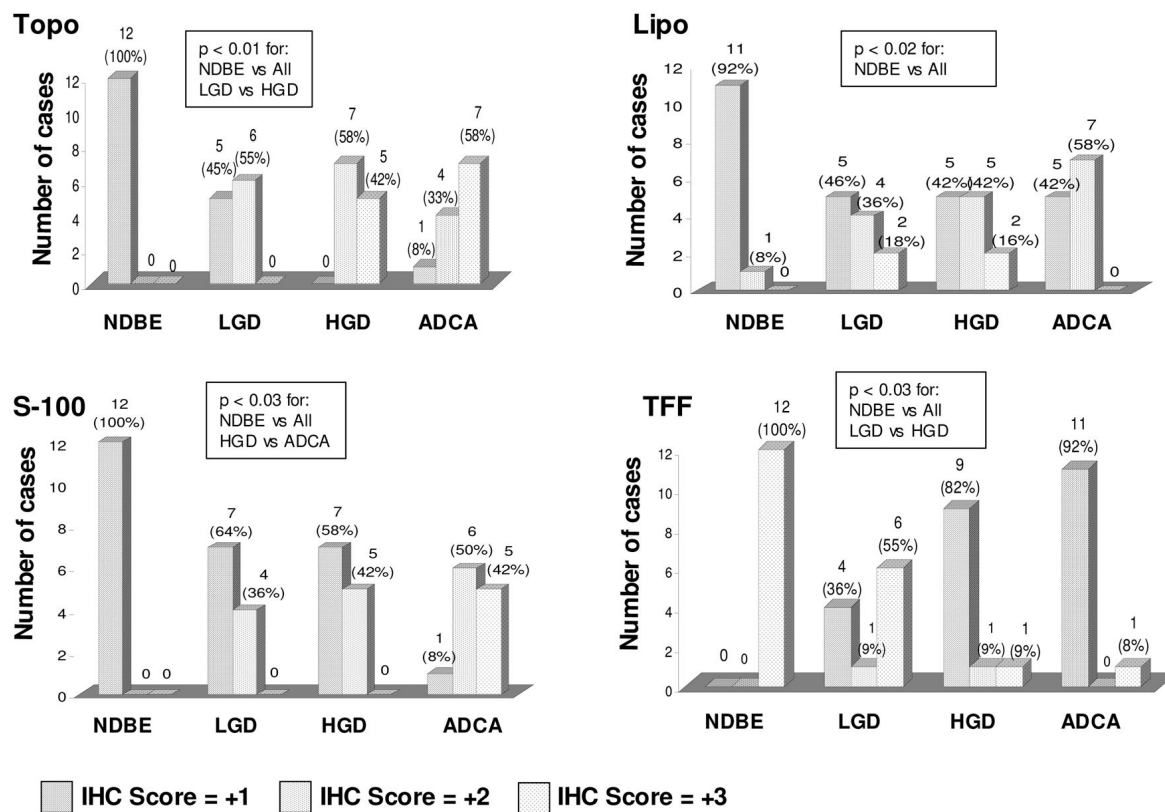


Figure 3A-H.

Immunohistochemical analysis of select proteins in biopsies of high grade dysplasia and non-dysplastic BE. All magnifications at 200x. 3A. Strong nuclear staining of surface dysplastic epithelium with topoisomerase II α . 3B. Nuclear staining seen only in the crypt region of non-dysplastic BE with topoisomerase II α . 3C. Patchy staining of dysplastic epithelium with S100A9. 3D. Negative staining of non-dysplastic BE with S100A9. 3E. Strong cytoplasmic staining of dysplastic epithelium with lipocalin-2. 3F. Negative staining of non-dysplastic BE with lipocalin-2. 3G. Negative staining of dysplastic epithelium with trefoil factor 1. 3H. Strong, diffuse staining of non-dysplastic BE with trefoil factor 1.

**Figure 4.**

Summary of immunohistochemical stains for topoisomerase II α . (Topo), lipocalin-2 (Lipo), S-100A9 (S-100) and trefoil factor 1 (TFF). Non-dysplastic BE (NDBE), low grade dysplasia (LGD), high grade dysplasia (HGD) and adenocarcinoma (ADCA).

Table 1
RT-PCR Primers for Confirmation of Microarray results

Name	Symbol	Genbank ID	Sense primer Anti sense primer	Amplicon
β Actin	<i>ACTB</i>	NM_001101	TCCCCCAACTTGAGATGTATGAAG AACTGGTCTCAAGTCAGGTACAGG	91
Alanyl (membrane) aminopeptidase (CD13)	<i>ANPEP</i>	NM_001150	AACCTCATCCAGGCAGTGAC AAGCCTGTTCTCTCGTTGTC	*92
Aldolase B, fructose bisphosphate	<i>ALDOB</i>	NM_000035	TGGCATCTGCTTTTGTCTG TTGGTAGAGGGCAAAGGTTG	*83
Calcium/Calmodulin-dependent protein kinase II inhibitor 1	<i>CAMK2N1</i>	N75559	ACGGCGGTAACAGTTATTGG TGATTTCATCGTGGGTAGCA	85
Complement component 3	<i>C3</i>	NM_000064	GGAGCAGTCAAGGTCTACGC GCTTCCATCCTCCTTTTCC	*82
Fatty acid binding protein 1, liver	<i>FABP1</i>	NM_001443	GCAGAGCCAGGAAAACCTTG CACCCCCTTGATATCCTTCC	*88
Fidgetin-like 1	<i>FIGNL1</i>	NM_022116.2	TGCACAGTACCTGGAGTGAAA GAGCTGGAGGTCTGCATTTT	*99
Formyl peptide receptor 1	<i>FPR1</i>	NM_002029	AAGACCACAGCTGGTGAACA AGCCAGCAGATACAGCAGGT	*101
Histone cluster 1,H2ag	<i>HIST1H2AG</i>	NM_021064	TGCCCCAAAAGACTGAGAGC CGTTGGTTTGGACTCGATT	95
Hydroxyprostaglandin dehydrogenase 15-(NAD)	<i>HPGD</i>	J05594	AAAAGAAGAAAACATGGGACAA CCATTGGCAATCAATGGTG	*99
Hydroxysteroid (17-β) dehydrogenase 2	<i>HSD17B2</i>	NM_002153	CACGAAGCCAGTGCAGATAA ATTGTTGATCACAGCCCACA	*85
Lipocalin-2	<i>LCN2</i>	NM_005564	CAAGGAGCTGACTTCGGAAC TACACTGGTCGATTGGGACA	*104
Meprin A, alpha	<i>MEP1A</i>	NM_005588	TTGTTGGCACTCAACAATGG TTTCATCATATATATTCAATCTGCAA	*104
Minichromosome maintenance complex component 10	<i>MCM10</i>	AL136840	TTGTTGTGGGAGATGGTTGA CCTTCCACCCAATTAGAGCA	*96
Matrix metalloproteinase 1	<i>MMP1</i>	NM_002421	AGGTCTCTGAGGGTCAAGCA CTGGTTGAAAAGCATGAGCA	*111
Matrix metalloproteinase 12	<i>MMP12</i>	NM_002426	AGGAATCGGGCCTAAAATTG TGGTGATACGTTGGAGTAGGAA	*110
Mucin 5AC	<i>MUC5AC</i>	AW192795	TCCTTCGAGTGCTTGTGTTG GCCTTTCAGCTACACGAGGT	82
Nurim (nuclear membrane envelope protein)	<i>NRM</i>	NM_014641	CATGGGCCTCAAACAGGTAT GCAGGTGGGAGAAGAGTCTG	*95
Protein phosphatase 2 (formerly 2A) catalytic subunit, β isoform	<i>PPP2CB</i>	AI379894	CGAGTGTAAGCAGCTGAACG CGAACCTCTTGACATTTGA	*93
Protein tyrosine phosphatase, non-receptor type 7	<i>PTPN7</i>	NM_002832	ACTTCTGGGAGATGGTGTGG GGGCCAGTAGTGGACACATT	*95
S100 calcium binding protein A9	<i>S100A9</i>	NM_002965	AGAAGATGCACGAGGGTGAC CACTGTGATCTTGGCCACTG	96
Secernin 1	<i>SCRN1</i>	NM_014766	ATTCTGCACAGTCCCAGGTC CACGAGAAATCTGCAGGTGA	107
TIA1 cytotoxic granule-associated RNA binding protein-like 1	<i>TIAL1</i>	NM_003252	TGAAGGACATGTGGTTAAATGC CCATACACTTGGCTCCATTG	*108
Trefoil factor 1	<i>TFF1</i>	NM_003225.2	CCCTCCAGAAGAGGAGTGTG CCGAGCTCTGGGACTAATCA	*101
Topoisomerase (DNA) IIα	<i>TOP2A</i>	AL561834	GCCCTCAAGAAGATGGTGTG TGCCAATGTAGTTTGTTCCTTG	*104

All primers were designed to amplify at the 3' end of their respective transcripts

*
Intron spanning primers.

Table 2

Differentially Expressed Genes Confirmed by Real-Time Quantitative PCR *

	Functional Gene Group	GeneBank ID	GeneChip Fold Change	p value
Upregulated genes				
Complement component 3	Miscellaneous	NM_000064	13.1	0.016
Topoisomerase (DNA) II α 170kDa	Cell proliferation and cell death	AL561834	12.6	0.01
Matrix metalloproteinase 1 (interstitial collagenase)	Extracellular matrix and protease	NM_002421	10.8	0.018
Matrix metalloproteinase 12 (macrophage elastase)	Extracellular matrix and protease	NM_002426	9.3	0.006
TIA1 cytotoxic granule-associated RNA binding protein-like 1	Cell proliferation and cell death	NM_003252	8.3	0.005
Protein tyrosine phosphatase, non-receptor type 7	Metabolism and mitochondria	NM_002832	7.3	0.010
Nurim (nuclear envelope membrane protein)	Cell adhesion, motility and membrane proteins	NM_014641	7	0.016
Histone cluster 1, H2ag	Nucleic acid binding and transcription factors	NM_021064	7	0.004
Lipocalin-2 (oncogene 24p3)	Ca ⁺ binding and ion channels	NM_005564	6.8	0.003
Fidgetin-like 1	Cell proliferation and cell death	AK023411	6.8	0.01
Protein phosphatase 2 (formerly 2A), catalytic subunit, β isoform	Cell proliferation and cell death	AI379894	6.7	0.003
Formyl peptide receptor 1	Cell adhesion, motility and membrane proteins	NM_002029	6.4	0.003
Minichromosome maintenance complex component 10	Cell proliferation and cell death	AL136840	6.3	0.005
Secernin 1	Miscellaneous	NM_014766	6	0.004
S100 calcium binding protein A9	Ca ⁺ binding and ion channels	NM_002965	4.1	0.003
Downregulated genes				
Fatty acid binding protein 1 liver	Metabolism and mitochondria	NM_001443	-2.5	0.003
Trefoil factor 1	Cell adhesion, motility and membrane proteins	NM_003225	-2.6	0.003
Mucin 5AC, oligomeric mucus/gel-forming	Extracellular matrix and protease	AW192795	-2.6	0.01
Aldolase B, fructose-bisphosphate	Metabolism and mitochondria	NM_000035	-2.8	0.003
Calcium/calmodulin-dependent protein kinase II inhibitor 1	Signal transduction	N75559	-3	0.006
Hydroxysteroid (17- β) dehydrogenase 2	Metabolism and mitochondria	NM_002153	-3.1	0.003
Hydroxyprostaglandin dehydrogenase 15-(NAD)	Metabolism and mitochondria	J05594	-3.3	0.004
Meprin A, alpha (PABA peptide hydrolase)	Extracellular matrix and protease	NM_005588	-4.7	0.003
Alanyl (membrane) aminopeptidase	Extracellular matrix and protease	NM_001150	-4.7	0.003

* See Supplemental Material for complete list of genes (fold change ≥ 2.5) listed by functional group